

RSC Advances



This is an *Accepted Manuscript*, which has been through the Royal Society of Chemistry peer review process and has been accepted for publication.

Accepted Manuscripts are published online shortly after acceptance, before technical editing, formatting and proof reading. Using this free service, authors can make their results available to the community, in citable form, before we publish the edited article. This *Accepted Manuscript* will be replaced by the edited, formatted and paginated article as soon as this is available.

You can find more information about *Accepted Manuscripts* in the [Information for Authors](#).

Please note that technical editing may introduce minor changes to the text and/or graphics, which may alter content. The journal's standard [Terms & Conditions](#) and the [Ethical guidelines](#) still apply. In no event shall the Royal Society of Chemistry be held responsible for any errors or omissions in this *Accepted Manuscript* or any consequences arising from the use of any information it contains.

Development of polyacrylamide chromium oxide as a new sorbent for solid phase extraction of As (III) from Food and Environmental water Samples.

Nafisur Rahman* and Uzma Haseen

*Department of Chemistry, Analytical Research division

Aligarh Muslim University,

Aligarh-202002 (U.P.), India.

Phone No. +91-9412501208

Email: nafisurrahman05@gmail.com

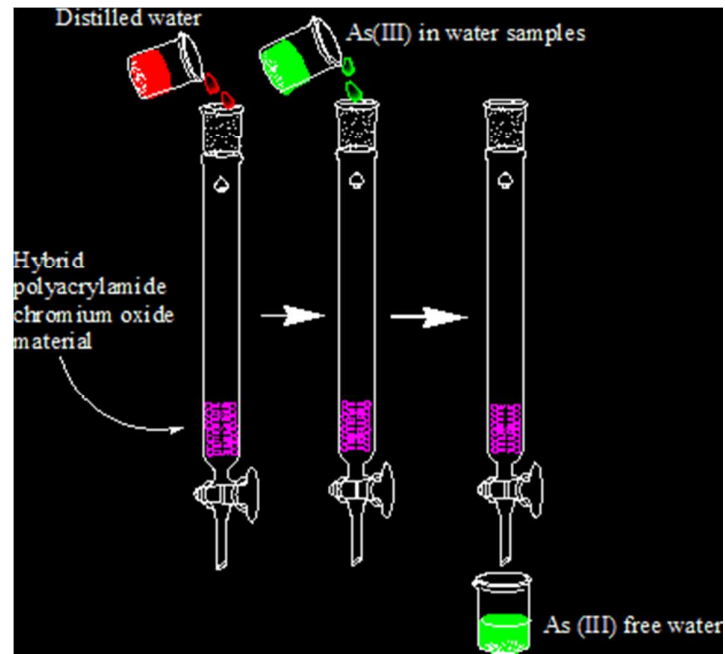
Department of Chemistry, Analytical Research division

Aligarh Muslim University,

Aligarh-202002 (U.P.), India

Email: uzma.haseen@gmail.com

Graphic for abstract:



ABSTRACT:

A new hybrid polyacrylamide chromium oxide (PACO) was synthesized and characterized by elemental analysis, x-ray diffraction (XRD), scanning electron microscopy (SEM) coupled with EDX, transmission electron microscopy (TEM), thermal and infrared spectral studies. The application of PACO as a solid phase extraction sorbent in environmental analysis is reported for the first time using arsenic as a model target. The sorption of As (III) onto PACO has been studied through batch and column techniques. The adsorption equilibrium data were analyzed by Langmuir and Freundlich isotherm models. The experimental data obeyed the pseudo second order kinetic model. The effects of adsorption and desorption conditions for arsenic (III) including initial pH of sample, solution volume and flow rate of sample solution; eluent and its flow rate were investigated and optimized prior to its determination by spectrophotometry and inductively coupled plasma-atomic emission spectrometry (ICP-AES). As (III) can be quantitatively retained on PACO over the pH range 6.5-7.5 from sample volume up to 500 mL and then eluted completely with 5 mL of 0.5 M HNO₃+NaNO₃. Under the optimal conditions, the enrichment factor was 100. The RSD values for day to day and column to column precision were found to be 3.91 % and 4.55% respectively, at 6 µgL⁻¹ As (III) level. The recoveries of arsenic in the environmental water samples were above 95 % with 500 mL water samples. The proposed method has been applied successfully to the analysis of total inorganic arsenic in water samples, basmati rice and tobacco cigarette.

KEYWORDS: Polyacrylamide chromium oxide, solid phase extraction, Arsenic (III), Environmental water, Rice, Cigarette Tobacco

1. INTRODUCTION

Arsenic is a toxic element and is widely distributed in the environment.^{1,2} The sources of arsenic in soil are mainly the rock materials from which it is derived.³ The major sources of arsenic in the environment are the smelting of ores of gold, silver, copper and others.⁴ Arsenic from these sources is distributed in soil, water and air. Arsenic enters drinking water mostly in the form of inorganic trivalent (arsenite, As (III)) and pentavalent (arsenate, As(V)) oxidation states from natural deposits in the earth or from agricultural and industrial practices.⁵ Arsenic contamination in groundwater has created a serious threat to human due to ingestion of arsenic in the human body through water and food.⁶ Exposure to arsenic has been linked to increased risk of lung disease, heart disease, cancer and reproductive disorder.⁷ Vegetables grown in arsenic rich soil and irrigated with arsenic contaminated ground water may contain higher amount of arsenic that may pose threat to consumers.⁸ It has been reported that rice has the ability to draw in arsenic from the soil without harming themselves. Thus the accumulation of arsenic in rice presents a health risk to humans who eat on a regular basis.⁹ Arsenic is also found in cured tobacco and mainstream cigarette.¹⁰ The level of arsenic in mainstream smoke is about 10.4 ng per cigarette.¹⁰ Different forms of arsenic species are known to have different toxicities.¹¹ Generally inorganic arsenic is more toxic than organic arsenic, and As (III) is much more toxic than As(V) because As (III) binds to single but with higher affinity for vicinal sulfhydryl groups that reacts with a variety of proteins and inhibits their activity.^{12,13} In view of the extreme toxicity of arsenic, World health organization, Environmental protection agency and the Central pollution control board have set 0.01 mg/L and 0.05

mg/L as the maximum permissible limit of arsenic in drinking water.¹⁴⁻¹⁶ Therefore, it is required to determine the arsenic species in contaminated water samples periodically.

The removal of arsenic from drinking water is becoming more and more urgent. Different methods such as chemical precipitation,¹⁷ coagulation and electrocoagulation,^{18,19} reverse osmosis,^{20,21} ion exchange,^{22,23} bioremediation^{24,25} and adsorption²⁶⁻²⁸ have been developed for removal of arsenic from aqueous solutions. Moreover, nanomaterials have also been tested for the removal of arsenic from contaminated water to make it potable and for other household utilities. Functionalized nanomaterials^{29, 30} are attractive because of their improved properties resulting from their synergistic and cooperative effects. Recently, acetate functionalized zinc oxide nanomaterials have been used for selective removal of arsenic from contaminated water.³¹ Composite materials, containing magnetic nanoparticle and cellulose, have been used for removal of arsenic.³² In addition, magnetite reduced graphene oxide composites show high binding capacity for As (III) and As(V) and hence used for arsenic removal from water.³³ It has been reported that As (III) occurs in very low concentrations in natural water which makes its direct determination difficult and hence pre-concentration step is required prior to its determination.³⁴ The determination of arsenic in waters was carried out using inductively coupled plasma-mass spectrometry,³⁵ atomic fluorescence spectrometry-hydride generation,³⁶ atomic absorption spectrometry-hydride generation³⁷ and inductively coupled plasma- atomic emission spectrometry.³⁸ But all these techniques are costly and require sophisticated handling. To the best of our knowledge until now, there is no simple and viable technique for the field determination of arsenic in aqueous environments.³⁹ Keeping this in view, a hybrid material was synthesized which has high affinity for As (III) and hence selectively binds with As (III) in presence of large number of foreign ions from environmental samples. Total inorganic arsenic was

determined as As (III) after reducing As(V) using simple spectrophotometric procedure and sophisticated ICP-AES.

In this manuscript, the preparation of polyacrylamide chromium oxide was reported. The material was characterized by FTIR, XRD, TGA, DTA, SEM with EDX and TEM. The practical utility of the material was explored based on column operation to investigate parameters for preconcentration of As (III) and its desorption. The As (III) was determined in water samples, basmati rice and cigarette tobacco

2. EXPERIMENTAL SECTION

2.1. Materials and Methods

All chemicals used were of analytical reagent grade. Acrylamide (Otto Chemie Pvt. Ltd., Mumbai, India), $\text{CrCl}_3 \cdot 6\text{H}_2\text{O}$, (Merck, Mumbai, India) and ammonia solution (Merck, Mumbai, India), were used for the synthesis of the material. Sodium arsenite and leucomalachite green was procured from Kemphasol (Mumbai, India) and Sigma-Aldrich (USA), respectively. The stock solution containing 1000 ppm As (III) was prepared by dissolving desired amount of sodium arsenite in distilled water. A solution containing 10 % potassium iodide and 10% ascorbic acid was prepared.

2.2. Instrumentation:

The synthesized polyacrylamide chromium oxide was characterized by using various analytical techniques. FTIR spectrums were recorded by FTIR spectrophotometer (Interspec 2020, Spectrolab, UK). The surface morphology of the material was examined using scanning electron microscope (JEOL JSM-6100, Japan) coupled with EDX technique. TEM images were also recorded using transmission electron microscope

(JEOL JSM 2100, Japan). X-ray diffraction (XRD) data were obtained by a diffractometer PW-3050/60 (X'PRO-PAN analytical, Netherland) with Cu K α radiation ($\lambda = 1.54\text{\AA}$). The thermogravimetric analysis was carried out with a DTG-60H thermal analyzer (DTG-60H, Shimadzu Corporation, Japan) in a nitrogen atmosphere at a heating rate of $10^\circ\text{C min}^{-1}$. An IRIS Intrepid II Model XPS Duo ICP-AES (Thermo Electron Corporation, Franklin, Mass. USA) and UV-1800 Spectrophotometer (Shimadzu, Japan) were used for the determination of arsenic.

2.3. Synthesis of polyacrylamide chromium oxide.

Chromium oxide was synthesized according to the previously described procedure.⁴⁰ For preparation of hydrous chromium oxide, 500 mL of 0.2M CrCl₃.6H₂O was taken in a conical flask and NH₄OH (6%) was added drop wise with continuous stirring till pH 6.0. The resulting green color precipitate was mixed with acrylamide and heated at $70\pm 2^\circ\text{C}$ for 8h with constant stirring and again kept for 24 h at room temperature. It was filtered and washed several times with distilled water and 0.01M HCl solution. Finally the gel was dried in an oven at 50°C . The dried material was broken into small granules on immersion in distilled water. Further the material was dried and sieved to obtain particles of desired size that is; mean radii $\approx 125\ \mu\text{m}$ (80-120 mesh). The fine particles of the material were treated with 0.5M HCl solution to convert the material in the Cl⁻ form. The excess Cl⁻ ion from the material was removed after several washings with distilled water and finally dried at 50°C .

2.4. Chemical Composition.

To determine the chemical composition of PACO, 0.10 g of the material was dissolved in a minimum volume of concentrated H₂SO₄ and then diluted to 100 mL with distilled

water. The amount of chromium was determined by atomic absorption spectrometer. The percentage of carbon, hydrogen and nitrogen was analyzed with the help of CHN analyzer.

2.5. Chemical Stability.

For determination of chemical stability, different 200 mg portions of PACO were kept in 25 ml of varying concentrations of HCl, HNO₃, H₂SO₄, HClO₄, and NaOH for 24 h with occasional shaking. The supernatant liquid was analyzed for chromium using an atomic absorption spectrometer. The leaching of Cr (III)/(VI) was also tested by passing 500 mL of water sample through the column packed with 1.0 g of PACO.

2.6. Ion-exchange/Sorption capacity.

For the determination of ion-exchange/sorption capacity of As (III), 0.5g of the dry polyacrylamide chromium oxide in Cl⁻ form was taken into a glass column having an internal diameter of 1 cm and fitted with glass wool support at the bottom. Sodium nitrate solution (1.0 M) was passed through the column at a slow flow rate (0.5 mL min⁻¹) to elute Cl⁻ ions completely and the effluent was titrated against standard 0.1 M AgNO₃ solution. The breakthrough capacity of PACO packed column (1.0g) for As (III) was determined by passing 200 mL of a sample solution containing 50 mg of As (III). The As (III) remaining in solution was measured by withdrawing 1.0 mL of the sample and subjected to spectrophotometric determination using leucomalachite green⁴¹ after appropriate dilution.

2.7. Batch Adsorption Experiment.

Batch adsorption experiments were carried out by adding 0.2g adsorbent with 50 ml of arsenic (III) solution in 100 mL stoppered conical flasks. The stoppers were used to avoid change in concentration due to evaporation. The mixture was agitated at 160 rpm in a thermostatic shaker until equilibrium was attained. After a predetermined contact time, the aqueous solution in each flask was filtered using 0.45 µm membrane filters and the arsenic

concentration in the filtrate was determined by spectrophotometry using leucomalachite green as a reagent. The experiments were carried out at variable pH (1-10), contact time (5-50 min), temperature (30-50°C) and initial concentration of As (III) (20-100 ppm). Under the optimum experimental conditions, the uptake of As (III) by the material was calculated using the expression:

$$q_e = \left(\frac{C_0 - C_e}{m} \right) V \quad (1)$$

where q_e is the equilibrium uptake (mg/g), C_0 is the initial concentration of As (III), and C_e is the concentration of As (III) at equilibrium, V is the volume of solution (L) and m is the mass of PACO (g).

2.8. Preconcentration procedure:

A glass column with an inner diameter of 1 cm and a length of 10 cm was filled with 2.0 g PACO in Cl⁻ form. Before packing the column, the hybrid material was thoroughly rinsed with distilled water, 500 mL standard or water samples containing arsenic was mixed with 5 mL of concentrated HCl and 2.5 mL of the KI-ascorbic acid solution to reduce As(V) to As (III).⁴² Then the solution pH was adjusted with NaOH solution to the desired value. The solution was passed through the column at a flow rate of 3.5 mL min⁻¹. Afterwards, the As (III) retained on the column was eluted with 5 mL of a mixture of 0.50 M HNO₃+ NaNO₃ at a flow rate of 0.5 mL min⁻¹. The effluent was analyzed for As (III) content by spectrophotometry and ICP-AES.

2.9. Collection and preparation of water samples:

The proposed method was evaluated for determination of total arsenic in synthetic standard water, tap water and river water samples. These samples were filtered through a

0.45 μm membrane and then As (V) was reduced to As (III) by treating with a solution containing KI and ascorbic acid. Afterward, the samples were subjected to the analysis.

2.10. Digestion of food samples.

Rice (polished & unpolished) and tobacco of cigarette were purchased from a local market (Aligarh, U.P., India). 1g of rice samples (polished and unpolished) and 1g tobacco of cigarette were digested separately, with 6.0 mL of concentrated HNO_3 (70%) and 2.0 mL of (25%) H_2O_2 on a hot plate, after digestion the sample is filtered and diluted to 20 mL with the distilled water.⁴³ Finally As (V) was reduced to As (III) by adding a solution containing KI and ascorbic acid and further diluted to 100 mL with distilled water and the amount of total arsenic was determined.

3. RESULTS AND DISCUSSION

Various samples of polyacrylamide chromium oxide, an anion exchanger, were prepared by sol-gel mixing of inorganic precipitate of hydrous chromium oxide and different volumes of 0.2 molL⁻¹ acrylamide with constant stirring at $70\pm 2^\circ\text{C}$. Table 1 shows the conditions of synthesis and ion exchange capacity for Cl^- ions. As can be seen from table that 100 mL of 0.2 M acrylamide was sufficient to give the stable structure with ion-exchange capacity of 1.46 meq/g. Further addition of acrylamide did not affect the ion exchange capacity of the material. Hydrous chromium oxide was also prepared under the same experimental conditions which exhibited an ion exchange capacity of 0.70 meq/g. Moreover, the hybrid material showed better ion exchange capacity, reproducible behavior and improved chemical and thermal stabilities with regard to hydrous chromium oxide. The improvement in these characteristics may be due to incorporation of polyacrylamide into inorganic moiety i.e., hydrous chromium oxide. The specific surface area of PACO was determined by nitrogen adsorption using the BET method and found to be 92.37 m²/g. Moreover, the breakthrough capacity was also evaluated by passing 200 mL sample

solution containing 50 mg of As (III) through a column packed with PACO. The breakthrough capacity was found to be 18.2 mg/g for As (III). This study suggested the good retention ability for preconcentration of As (III) species.

The chemical stability of the sorbents is one of the important parameters that are required for suitability for column operation. The chemical resistivity of PACO was evaluated in different concentrations of HCl, HNO₃, H₂SO₄, HClO₄ and NaOH solutions. The experimental results revealed that PACO is fairly stable in 1M solutions of HCl, HNO₃, H₂SO₄, and HClO₄ and 0.1 M NaOH. Moreover, no traces of chromium were found in such solutions. The mechanical stability studies with water and 0.5 M HNO₃+NaNO₃ were performed by using a high pressure peristaltic pump with a flow rate of 10 mL/min. The column packed with 125 μm particles of PACO was placed in a water jacketed column to maintain a temperature of 30°C, and used to determine the pressure drop in the sorbent. It was observed that the results of pressure test (100 psi) did not significantly change, indicating the material has strong mechanical stability for column operation.

The fourier transform infrared (FTIR) spectrum of polyacrylamide chromium oxide is shown in Fig. 1. The absorption peak in the range 3500-3200 cm⁻¹ indicates the presence of OH group. The -NH stretching was also observed at 3500 cm⁻¹ as a weaker band. Further the presence of a peak at 1633 cm⁻¹ may be assigned to C=O stretching vibration. Another peak observed at 1554 cm⁻¹ may be attributed to amide II band which is due to a motion combining both the N-H bending and C-N stretching vibrations of the group CO-NH-. The peak appearing at 1396 cm⁻¹ indicates the CH₂ symmetric scissoring. The presence of peak at 534 cm⁻¹ is due to Cr-O bonding. The thermal analysis of sample PACO is presented in Fig. 2. The weight loss occurred in three distinct stages: (a) 14.2% weight loss was observed in the temperature range 30-170 °C (b) 6.25% weight loss occurred in the temperature range 170-340°C and (c) the structural deformation occurred in

the temperature range 340-456 °C. Above 456 °C, the weight of the material became constant, indicating the formation of chromium oxide. The data of TGA can be correlated with differential thermal analysis (DTA). The endothermic peak was noticed at 170 °C which indicates the loss of water molecule present in the free or bonded form in the matrix. DTA curve shows two exothermic peaks. The first exothermic peak was noticed at 310.34 °C which indicated the loss of the amide group in the form of ammonia.⁴⁴ Another exothermic peak at 424.50 °C indicated the decomposition of organic molecules in the material. Therefore, the thermogravimetric analysis strongly indicated the presence of polyacrylamide in the matrix.

The SEM images of hydrous chromium oxide and polyacrylamide chromium oxide are shown in Fig. 3(a-c). There is a remarkable change in morphology and structure when polyacrylamide was incorporated into hydrous chromium oxide. In case of PACO (Fig.3b) polyacrylamide might bind with hydrous chromium oxide regularly and effectively. SEM image (Fig. 3c) shows the white spots distributed over the surface which resulted from the adsorption of As (III) on the adsorbent. To further investigate the sorption of As (III) on PACO, energy dispersive spectroscopy (EDS) mapping was performed and the results are shown in Fig.4. The EDX spectrum clearly shows the presence of C,O,N,Cr and As (III) on the As (III) sorbed PACO. The transmission electron micrographs (TEM) of hydrous chromium oxide, PACO and As (III) sorbed PACO are shown in Fig. 5(a-c). It is evident from the figure that polyacrylamide was successfully incorporated inside the inner sphere of hydrous chromium oxide and hence expected that the material would show stronger chemical stability and activity than hydrous chromium oxide. X-ray diffraction pattern (Fig. 6) of PACO showed very small intensity peaks which suggested the amorphous nature of the material.

The combining mole ratio of chromium and acrylamide was ascertained on the basis of chemical and elemental analysis of polyacrylamide chromium oxide. The percentage composition of PACO was found as: Cr (28.24%), C (19.57%), N (7.60%), H (4.49%) and others (39.11%). On the basis of these results the molar combining ratio between Cr and acrylamide was found to be 1:1. It is reported that Cr(III) forms several hydroxo species such as Cr(OH)^{2+} , Cr(OH)_2^+ , Cr(OH)_3 and Cr(OH)_4^- . In the present study, Cr(OH)_3 was precipitated on addition of NH_4OH which is represented by the following equilibrium in solution phase:⁴⁵



Under the experimental conditions, Cr(OH)_2^+ reacted with acrylamide to form polyacrylamide chromium oxide (scheme 1). It is evident from TGA curve that 14.2% weight loss is due to the removal of $n\text{H}_2\text{O}$ molecule. Considering the above structure, the value of 'n' the external water molecule, was calculated by using the Alberti's equation:⁴⁶

$$18n = \frac{x(M+18n)}{100} \quad (2)$$

Where x and $(M+18n)$ represent the percent weight loss (14.2%) and molecular weight of the material, respectively. The value of 'n' was found to be 1.44 per mole of the material.

3.1. Batch Method

The uptake of As(III) onto PACO was optimized with respect to key parameters such as pH, initial concentration of As(III), contact time and temperature. It was observed that maximum retention of As(III) was in the pH range 6.5-7.5 and hence all subsequent experiments were carried out at pH 6.8. The effect of contact time on the retention of As(III) was studied by shaking 50 mL of 100 mgL^{-1} As(III) solution at an initial pH 6.8 with 0.2 g PACO. The

contact time was varied from 5 to 50 min. At the first stage of 15 min, the rate of adsorption was fast due to the availability of a large number of surface sites and 78 % As(III) was removed. However, the adsorption gradually became slower until it reaches equilibrium (40 min). Hence 40 min contact time was selected for equilibrium studies. The effect of initial concentration of As(III) on the adsorption was examined. It was observed that the extent of adsorption increases with increase in concentration from 20 to 100 mgL⁻¹.

3.1.1. Adsorption Isotherms.

The adsorption isotherm was studied in order to understand the interactive behavior between adsorbate and adsorbent and to design the adsorption systems. In this study the experimental data of As (III) adsorption were analyzed by Langmuir and Freundlich models.

Langmuir Model is based on the assumption that the adsorbed layer is one molecule in thickness i.e., monolayer adsorption; the adsorption can occur at fixed number of sites with equivalent energy and no interaction between the molecules.⁴⁷ The linear equation that describes the Langmuir model is given as:

$$\frac{1}{q_e} = \left(\frac{1}{q_m K_L} \right) \frac{1}{C_e} + \frac{1}{q_m} \quad (3)$$

Where C_e is the equilibrium concentration (mg/L), q_e is the amount of solute adsorbed per unit mass of adsorbent (mg/g), the parameter q_m and K_L are the maximum adsorbent capacity (mg/g) and adsorption binding constant (Lmg⁻¹), respectively. The values of q_m and K_L were calculated from the slope and intercept of the linear plots of $1/q_e$ Vs $1/C_e$ (Fig. 7) and isotherm parameters are reported in Table 2. The essential features of Langmuir adsorption isotherm parameter can be used to predict the affinity between adsorbate and adsorbent by a dimensionless equilibrium parameter, R_L , which is defined by

$$R_L = \frac{1}{1+K_L C_o} \quad (4)$$

Where C_o denotes the initial concentration of As (III). The value of R_L suggested the nature of adsorption. The R_L value between 0 and 1 indicates the favorable adsorption.⁴⁸ In this study, the values of R_L were in the range 0.075-0.289, 0.054-0.220 and 0.050-0.210 at 303K, 313K and 323K, respectively, which indicated that the adsorption of As (III) onto PACO is favorable at all the temperatures studied.

Freundlich isotherm model can be applied onto heterogenous surfaces involving multilayer sorption. The linear form of Freundlich isotherm can be expressed as:⁴⁹

$$\ln q_e = \ln K_f + \frac{1}{n} \ln C_e \quad (5)$$

Where K_f is a constant related to the adsorption capacity and 'n' is an empirical parameter related to the intensity of adsorption. The values of K_f and n were calculated from intercept and slope of linear plots of $\ln q_e$ versus $\ln C_e$ (Fig. 7) and reported in Table 2. If the value of $n > 1$, then the adsorption is favourable.⁵⁰ In present investigation, the value of n was found to be in the range 1.14-1.40.

3.1.2. Adsorption Kinetics:

In order to understand the process of adsorption of As (III) onto PACO, pseudo-first order and pseudo-second order kinetic models were applied to analyze the experimental data. The pseudo-first order kinetic model is expressed as:⁵¹

$$\log(q_e - q_t) = \log q_e - \frac{k_1}{2.303} t \quad (6)$$

Where q_e and q_t are the amounts of As (III) adsorbed per unit mass of adsorbent at equilibrium and at time t respectively; k_1 (min^{-1}) is the rate constant of pseudo first order adsorption process. The pseudo-first order kinetic model parameters for As (III) adsorption were calculated (Table 3) from the plot of $\log(q_e - q_t)$ Vs. t (Fig. 8). The linear

regression coefficient (R^2) gave a poor fitting ($R^2 < 0.916$) which suggested that the adsorption of As (III) on PACO did not follow the pseudo first order rate equation. The pseudo-second order kinetic model is given below:⁵²

$$\frac{t}{q_t} = \frac{1}{k_2 q_e^2} + \frac{t}{q_e} \quad (7)$$

Where k_2 is the pseudo-second-order rate constant ($\text{gmg}^{-1}\text{min}^{-1}$). The plots of t/q_t Vs. t gave a straight line for As (III) at 303, 313 and 323 K (Fig. 9). The parameters of pseudo-second order kinetic model are summarized in table 3. The linear regression coefficient value (R^2) gave a better fitting ($R^2 > 0.999$) and sorption capacity calculated from the pseudo-second order model was found to be more consistent with the experimental sorption capacity. This finding suggests that the adsorption of As (III) onto PACO can be described by using pseudo-second order kinetic model.

3.2. Optimization for the solid-phase extraction of As (III).

3.2.1. Effect of pH:

The effect of pH on the uptake of As (III) ions was examined in the pH range of 3-10 by adjusting the pH of the model solution with HNO_3 or NaOH solutions. The proposed procedure was applied and the results are shown in Fig. 10. The figure shows that the arsenic (III) adsorption efficiency increased from 9.8 % to 62.0 % when the initial pH increased from 3.0 to 6.0. The maximum adsorption occurred in the pH range 6.5 to 7.5. The arsenic (III) adsorption efficiency rapidly decreased when initial pH was increased above 7.5. The arsenic (III) speciation as a function of pH shows that the deprotonation of H_3AsO_3 occurs at $\text{pH} > 8$. Therefore, the As (III) can be detected at the original pH of natural water samples at $\text{pH} \sim 7$ to 8 which is convenient for monitoring purposes. At $\text{pH} > 7.5$, the decrease in uptake of As (III) could be mainly due to two factors: (i) the electrostatic repulsion between As (III) ion and negatively charged surface of

polyacrylamide chromium oxide hybrid material and (ii) competition for active sites by excess amounts of hydroxyl ions. Hence, pH 6.8 was selected as an optimum value for extraction of As (III) onto PACO.

3.2.2. Sorption Mechanism.

The mechanism for the uptake of As (III) onto PACO has been proposed on the basis of results obtained from experimental investigations. The positive charge developed by $-\text{NH}_2$ group served as exchange site. The possible ion-exchange mechanism is shown in scheme 2. Similar observations have also been reported due to interaction between cationic $-\text{NH}_3^+$ group and anionic contaminants.⁵³ In addition the uptake of As (III) may take place through the interaction between surface $-\text{OH}$ group and unionized H_3AsO_3

3.2.3. Effect of sample solution flow rate and volume.

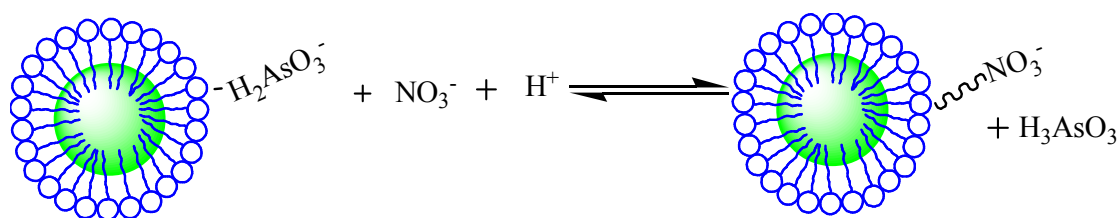
The effect of the sample flow rate on retention of As (III) on PACO was studied from 0.5 to 5.0 mL min^{-1} using aliquots of 500 mL of As (III) solution having a concentration of $10\mu\text{gL}^{-1}$. It was observed that the satisfactory results were obtained with flow rates of 3.5 mL min^{-1} . The adsorption of As (III) decreased when the flow rate was above 3.5 mL min^{-1} . This phenomenon can be explained on the basis of insufficient residence time of the solute in the column. As the flow rate was increased above 3.5 mL, the insufficient residence time caused a decrease in the bonding capacity of As (III) with the functional groups of the adsorbent. Therefore, considering the sensitivity 3.5 mL min^{-1} was chosen as the optimum flow rate for subsequent experiments. The experiments were carried out using different sample volumes (50,100, 200, 300, 400, 500, 550, 600 and 700 mL) with the same As (III) concentration of $10\mu\text{gL}^{-1}$. The breakthrough was considered to occur when the recovery was above 98 %. The results showed that the stable recoveries above 98 % were obtained when the sample volumes ranged from 50 to 550 mL. However, a

significant decrease in the recovery of As (III) (< 90 %) was obtained when the sample volume increased to 700 mL, so the breakthrough volume for As (III) was about 550 mL (Fig. 11). Therefore, 500 mL was selected as optimal sample volume for obtaining maximum enrichment factor. In addition, the treated water was analyzed for chromium content. The results showed that chromium was not leached in the treated water.

3.2.4. Effect of eluent flow rate and volume.

In order to get satisfactory elution with high enrichment factor, a series of experiments were performed to elute the adsorbed As (III) using HNO₃, NaNO₃, HCl, NaCl and mixed solutions of HNO₃ and NaNO₃ with concentration and volume ranges between 0.1-1.0 M and 1.5-6.0 mL, respectively. The results revealed that 5.0 mL of mixed solution of HNO₃ and NaNO₃ with equal concentration of 0.5 M was sufficient for the quantitative elution of As (III). The effect of eluent flow rate in the recovery of As (III) was also examined using 0.5M HNO₃ + NaNO₃ solution and varying the flow rate in the range of 0.2-3.0 mLmin⁻¹. The results revealed that a flow rate of 0.5 mL min⁻¹ was sufficient for quantitative recovery of As (III). Therefore, all the subsequent experiments were performed using 5 mL of 0.5 M HNO₃+NaNO₃ as eluent with a flow rate of 0.5 mL min⁻¹.

In the present study, nitrate ion is able to convert the adsorbent into the active forms and H⁺ helps to desorb As (III) as H₃AsO₃. The elution mechanism can be presented as follows:



3.2.5. Effect of Co-existing ions.

The effect of various foreign ions at the microgram level on sequestration of arsenic (III) onto PACO was investigated using column method. The tolerance limits of interfering species were established at the concentration that do not cause $>\pm 1.0$ % error in determination of arsenic (III). The interference of each foreign specie was evaluated by spiking synthetic samples containing $5 \mu\text{gL}^{-1}$ and $10 \mu\text{gL}^{-1}$ of the potential interfering specie and determining the As (III) concentration by spectrophotometry. Arsenic (III) recoveries ranged from 96.0 to 100 % for individual solutions spiked with different foreign ions. The results are summarized in Table 4.

3.3. Analytical performance.

Under the optimum conditions, the proposed enrichment procedure with PACO provides a linear analytical curve in the range $2.0\text{-}12.0 \mu\text{gL}^{-1}$ for determination of As (III) with a correlation coefficient of 0.9998 by spectrophotometry. The limits of detection and quantification were calculated based on three and ten times of the standard deviation of the blank solution measurements and found to be $0.45 \mu\text{gL}^{-1}$ and $1.38 \mu\text{gL}^{-1}$, respectively. Three replicate determinations at $6 \mu\text{gL}^{-1}$ and $10 \mu\text{gL}^{-1}$ As (III) concentration levels were carried out using three columns (i.e. three columns for each concentration) to test the reproducibility among the columns. The RSD values were found to be 3.91 % and 2.74 % from preconcentration and determination of $6 \mu\text{gL}^{-1}$ and $10 \mu\text{gL}^{-1}$, respectively on the day to day basis while RSD values were 4.55 and 3.15 for column to column (Table 5). It is evident from the experimental results that RSD of day to day and column to column is less than 5 %, indicating the satisfactory reproducibility among the columns. Under the optimized experimental conditions, water samples (500 mL) containing $5 \mu\text{gL}^{-1}$ each of As (III) and As(V) were mixed with 5 mL of concentrated HCl and 2.5 mL of KI-ascorbic acid solution to reduce As(V) to As (III). The recoveries of total arsenic from the resulting

solution were investigated. The recovery of total arsenic as As (III) was 99.24 ± 2.24 %. This confirms the ability of the method to determine the total inorganic arsenic.

3.4. Application to environmental water and food samples:

As an illustration of analytical application, the proposed preconcentration method was applied for the determination of As (III) in the pre-treated sample solutions. A sample solution of 500 mL (100 mL for rice and cigarette tobacco samples) was passed through the column at a flow rate of 3.5 mL min^{-1} and sorbed As (III) was eluted with 5 mL of 0.5 M $\text{HNO}_3 + \text{NaNO}_3$ at a flow rate of 0.5 mL min^{-1} . The effluent was collected and As (III) was determined by ICP-AES. The results are summarized in Table 6. The experimental results have proved that PACO can be an excellent solid phase extraction sorbent for As (III) pre-treatment and enrichment from real samples of water, rice and cigarette tobacco.

3.5. Comparison of adsorption capacity with other adsorbent for As (III) removal.

The arsenic (III) adsorption performance of PACO has been assessed by comparing the adsorption capacity with some literature available data. As can be seen in Table 7 that PACO has the adsorption capacity of 22.48 mgg^{-1} while the adsorbents such as Fe_3O_4 -reduced graphene oxide (RGO) nanoparticles, Fe_3O_4 -RGO- MnO_2 nanoparticles, NZVI-activated carbon nanoparticles and polymer supported Mn/Fe oxides showed an adsorption capacity of 13.1, 14.04, 18.2 and 13.5 mgg^{-1} , respectively. All other adsorbents mentioned in table 7 possess adsorption capacity less than 10 mgg^{-1} . Hence PACO has great potential for the removal of As (III) from aqueous solutions.

4. Conclusion:

In this study, polyacrylamide chromium oxide was developed as solid phase extraction sorbent for As (III) using column method. The current investigation has demonstrated well

the potential of PACO as sorbent for enriching of As (III). The breakthrough capacity of PACO for As (III) was found to be 18.2 mgg^{-1} . This method offers the advantages of simplicity, high enrichment factor, low limit of detection and low cost. Under the optimal condition, the detection limit and enrichment factor were found to be $0.45 \mu\text{gL}^{-1}$ and 100, respectively. The proposed method has been successfully used for As (III) enrichment in environmental water and food samples with good recoveries and precision.

- **Acknowledgments:**

The authors are thankful to UGC (DRS-II) and DST (FIST and PURSE) for facilities to carry out this work. One of the authors (Uzma Haseen) is grateful to UGC for providing financial support to complete the research work. We are also thankful to USIF, A.M.U. Aligarh for SEM and TEM. SAIF, Punjab University, Chandigarh for XRD and SAIF STIC Kochi Cochin for ICP-AES analysis.

References:

- (1) IPCS, Arsenic, World health organization, *International programme on chemical safety, Poison information monographs*, No4042, Geneva, 1999.
- (2) Agency for toxic substances and diseases registry, *Toxicological profile for arsenic* (Update), U.S. Public health service, U.S. Department of health and Human services, Atlanta, GA, 2007.
- (3) S. Wang and C.N. Mulligan, *Sci. Total Environ.*, 2006, **366**, 7001-721.
- (4) L. Jarup, and G. Pershagen, *Am. J. Epidemiol.*, 1991, **134**, 545-551.
- (5) J. C. Saha, A. K. Dikshit, M. Bandyopadhyay and K. C. Saha, *Environ. Sci. Technol.*, 1999, **29**, 281-298.
- (6) S. Sambu and R. Wilson, *Toxicol. Ind. Health*, 2008, **24**, 217-226.
- (7) IARC, *Some metals and metallic compounds* (IARC monographs on the evaluation of carcinogenic risk to humans) *International agency for research on cancer*, Lyon, France, 2004, **84**.
- (8) Science communication Unit, University of the West of England, Bristol, *and Science for Environment policy In-depth Report: Produced for the European Commission DG Environment*, Sept.2013. <http://ec.europa.eu/science-environment-policy>.
- (9) C.O. Akinbile, and A.M.M. Haque, *Trends Appl. Sci. Res.*, 2012, **7**, 331-349.
- (10) P.X. Chen and S.C. Moldoveanu, *Beitr. Tabakforsch Int.*, 2003, **20**, 448-458.
- (11) C.O. Abernathy, D.S. Thomas and R.L. Calderon, *J. Nutr. Biochem.*, 2003, **133**, 15365-15385.
- (12) F.W. Pontius, K.G. Brown and C.J. Chen, *J. Am. Water Work Assoc.*, 1994, **86**, 52-63.

- (13) H.V. Aposhian, R.M. Maiorino, R.C. Dart and D.F. Perry, *Clin. Pharmacol. Therap.*, 1989, **45**, 520-526.
- (14) World Health Organization. *Exposure to Arsenic a Major Public Health Concern*. WHO Document Production Services, Geneva, Switzerland, 2010.
- (15) Environmental Pollution Agency, *Environmental Pollution Control Alternatives*, EPA/625/5-90/025, EPA/625/4-89/025, Cincinnati, U.S. 1990.
- (16) M. J. Maushker, *Guidelines for water quality monitoring, central pollution control board* (A Government of India Organization). Delhi, India, 2010.
- (17) S. K. Tiwari and V. K. Pandey, *Recent Res. Sci. Technol.*, 2013, **5**, 88-91.
- (18) E. Lacasa, C. Saez, P. Canizares, F. J. Fernandez and M.A. Rodrigo, *Sep. Sci. Technol.*, 2013, **48**, 508-514.
- (19) P.D. Angel, G. Carreno, J.L. Nava, M.T. Matinez and J. Ortiz, *Int. J. Electrochem. Soc.*, 2014, **9**, 710-719.
- (20) P. Xu, M. Capito, and T.Y. Cath, *J. Hazard. Mater.*, 2013, **260**, 885-891.
- (21) M. Kang, M. Kawaski, S. Tamanda, T. Kamei and Y. Magara, *Desalination*, 2000, **131**, 293-298.
- (22) P. Pillewan, S. Mukherjee, A. K. Meher, S. Rayalu and A. Bansiwala, *Environ. Prog. Sust. Energy*, 2014, DOI: 10.1002/ep.11933
- (23) M. A. Barakat and S. Ismat-Shah, *Arabian J. Chem.*, 2013, **6**, 307-311.
- (24) S. Alvarado, M. Guedez, M.P. Lue-Meru, G. Nelson, A. Alvaro, A.C. Jesus Z. Gyula, *Bioresour. Technol.*, 2008, **99**, 8436-8440.
- (25) M. A. K. Azad, L. Amin and N.M. Sidik, *Chin. Sci. Bull.*, 2014, **59**, 703-714.
- (26) S. Mandal, M. K. Sahu and R. K. Patel, *Water Resources and Industry*, 2013, **4**, 51-67.

- (27) J. Qiao, Z. Cui, Y. Sun, Q. HU and X. Guan, *Front. Environ. Sci. Eng.*, 2014, **8**, 169-179.
- (28) S. Yao, Z. Liu and Z. Shi, *J. Environ. Health Sci. Eng.*, 2014, **58**, 1-8.
- (29) R. F. Balderas-Valdez and V. Agarwal, *Nanoscale Res. Lett.*, 2014, **9**, 1-6.
- (30) R. Chalasani and S. Vasudevan, *J. Mater. Chem.*, 2012, **22**, 14925-14931.
- (31) N. Singh, S.P. Singh, V. Gupta, H.K. Yadav, T. Ahuja, and S.S. Rashmi, *Environ. Prog. Sust. Energy*, 2013, **32**, 1023-1029.
- (32) X. Yu, S. Tong, M. Ge, J. Zuo, C. Cao and W. Song, *J. Mater. Chem., A* 2013, **1**, 959-965.
- (33) V. Chandra, J. Park, Y. Chun, J. Lee, I-C. W. Hwang and K.S. Kim, *ACS Nano*, 2010, **4**, 3979-3986.
- (34) N.B. Issa, V.N. Rajakovic-Ognjanovic, B.M. Jovanovich and L.V. Rajakovic, *Anal. Chim. Acta*, 2010, **673**, 185-193.
- (35) F. Ko and M. Yang, *J. Anal. Atomic Spec.*, 1996, **11**, 413-420.
- (36) P.C. Montesinos, M.L. Cervera, A. Paster, and M. de-la Guardia, *Talanta*, 2003, **60**, 787-799.
- (37) H. Narasaki, *Fresenius Z. Anal. Chem.*, 1985, **321**, 464-466.
- (38) J. Rayan and M. Clark, *Concordia Coll. J. Anal. Chem.*, 2010, **1**, 34-41.
- (39) A. Pillai, G. Sunita and V. K. Gupta, *Anal. Chim. Acta*, 2000, **408**, 111-115.
- (40) J. Iqbal, M.L. Mirza, M. Gul and K. Rahim, *J. Chem. Soc. Pak.*, 1991, **13**, 99-102.
- (41) H.D. Revanasiddappa, B.P. Dayananda and T.N.K. Kumar, *Environ. Chem. Lett.*, 2007, **5**, 151-155.
- (42) J. Kawalska, E. Stryjewska, P.Szymanski and J. Golimowski, *Electroanalysis*, 1999, **11**, 1301-1304.

- (43) O. D. Uluzlu, M. Tuzen, D. Mendil and M. Soylak *Food and Chem. Toxicol.*, 2010, **48**, 1393-1398.
- (44) S.A. Sadeek M.S. Refet and S.M. Taleb, *J. Korean chem. Soc.*, 2004, **48**, 358-366.
- (45) L. Spiccia and W. Marty, *Inorg. Chem. ACS*, 1986, **25**, 266-271.
- (46) G. Alberti, and E. Torracca, *J. Inorg. Nucl. Chem.*, 1968, **30**, 3075–3080.
- (47) I. Langmuir, *J. Am. Chem. Soc.*, 1916, **38**, 2221-2295
- (48) A. Ramesh, H. Hasefgawa, W. Sugimoto, T. Maki and K.Ueda, *Bioresour. Technol.*, 2008, **99**, 3801-3809.
- (49) H.M.F. Freundlich, *Z. Phys. Chem.*, 1906, **57**, 385-470.
- (50) S. Kamsonlian, S. Suresh, V. Ramanaia, C.B. Majumdar, S. Chand and A. Kumar, *Int. J. Sci. Technol.*, 2012, **9**, 565-578.
- (51) S. Lagergren, *Kungl. Sven. Ventenskapsakad. Handl.*, 1898, **24**, 1-39.
- (52) Y.S. Ho and G. Mckay, *Process Biochem. (Oxford U.K.)*, 1999, **34**, 451-465.
- (53) Y. Lee, W. Park and J. Yang, *J. Hazard. Mater.*, 2011, **190**, 652-658.
- (54) S.R. Kanel, B. Maming and L. H. C. Choi, *Environ. Sci. Technol.*, 2005, **39**, 1291-1298.
- (55) J. Hlavey and K. Polyak, *J. Colloid Interface Sci.*, 2005, **284**, 71-77.
- (56) B. Tatineni and M. Hideyuki, *Anal. Sci.*, 2002, **18**, 1345-1349.
- (57) Y. Chammui, P. Sooksamiti, W. Naksata and O-A. Arqueropanyo, *J. Chil.Chem. Soc.*, 2014, **59**, 2378-2381.
- (58) S.A. Baig, T.T. Sheng, C. Sun, X. Xue, L.Tan and X. XU, *PLOS ONE*, **9**(6), 2014: e100704:doi: 10.1371/journal.pone.0100704.
- (59) Y. Tian, M.Wu, X.Lin, P.Haung and Y.Huang, *J. Hazard. Mater.*, 2011, **193**, 10-16.
- (60) V.Chandra, J. Park, Y. Chun, J.W. Lee, I-C. Huang and K.S. Kim, *ACS Nano*, 2010, **4**, 3979-3986.

- (61) X. Luo, C. Wang, S. Luo, R. Dong, X. Tu, and G. Zeng, *Chem. Eng. J.*, 2012, **187**, 45-52.
- (62) H. Zhu, Y. Jia, X. Wu and H. Wang, *J. Hazard. Mater.*, 2009, **172**, 1591-1596.
- (63) I. J. Sobala, D. Ociniński and E. K. Balawejder, *Ind. Eng. Chem. Res.*, 2013, **52**, 6453-6461.

Figure Caption:

- Fig.1.** FT-IR spectrum of (a) Chromium oxide, (b) polyacrylamide chromium oxide.
- Fig. 2.** TGA-DTA curve of polyacrylamide chromium oxide.
- Fig. 3.** Scanning electron micrographs (SEM) (a) hydrous chromium oxide (HCO) and (b) polyacrylamide chromium oxide and (c) polyacrylamide chromium oxide As(III) loaded material.
- Fig. 4.** EDX spectrum of (a) chromium hydrous oxide, (b) polyacrylamide chromium oxide, and (c) As (III) sorbed PACO.
- Fig. 5.** TEM images; (a) hydrous chromium oxide, (b) As (III) loaded hybrid material, (c) wire type polymeric networking of polyacrylamide on hydrous chromium oxide surface.
- Fig. 6.** XRD of Polyacrylamide chromium oxide material
- Fig. 7.** (A) Langmuir, (B) Freundlich, isotherm plots for adsorption of As (III) onto PACO; (dosage of adsorbent, 0.2 g, contact time, 45 min, pH=6.8; volume, 50 mL)
- Fig. 8.** Pseudo- first order kinetic model for As (III) adsorption on polyacrylamide chromium oxide at different temperature.
- Fig.9.** Pseudo-second order kinetic model for As (III) adsorption on polyacrylamide chromium oxide at different temperature.
- Fig. 10.** Effect of pH on the sorption of As (III) onto PACO.
- Fig.11.** Effect of sample volume on recoveries of arsenic. Concentration; $10 \mu\text{gL}^{-1}$, pH; 6.8. flow rate 3.5 mL min^{-1} .
- Scheme 1.** Formation of polyacrylamide chromium oxide hybrid material under optimal synthesis conditions.
- Scheme 2.** Sorption mechanism of As (III) onto PACO.

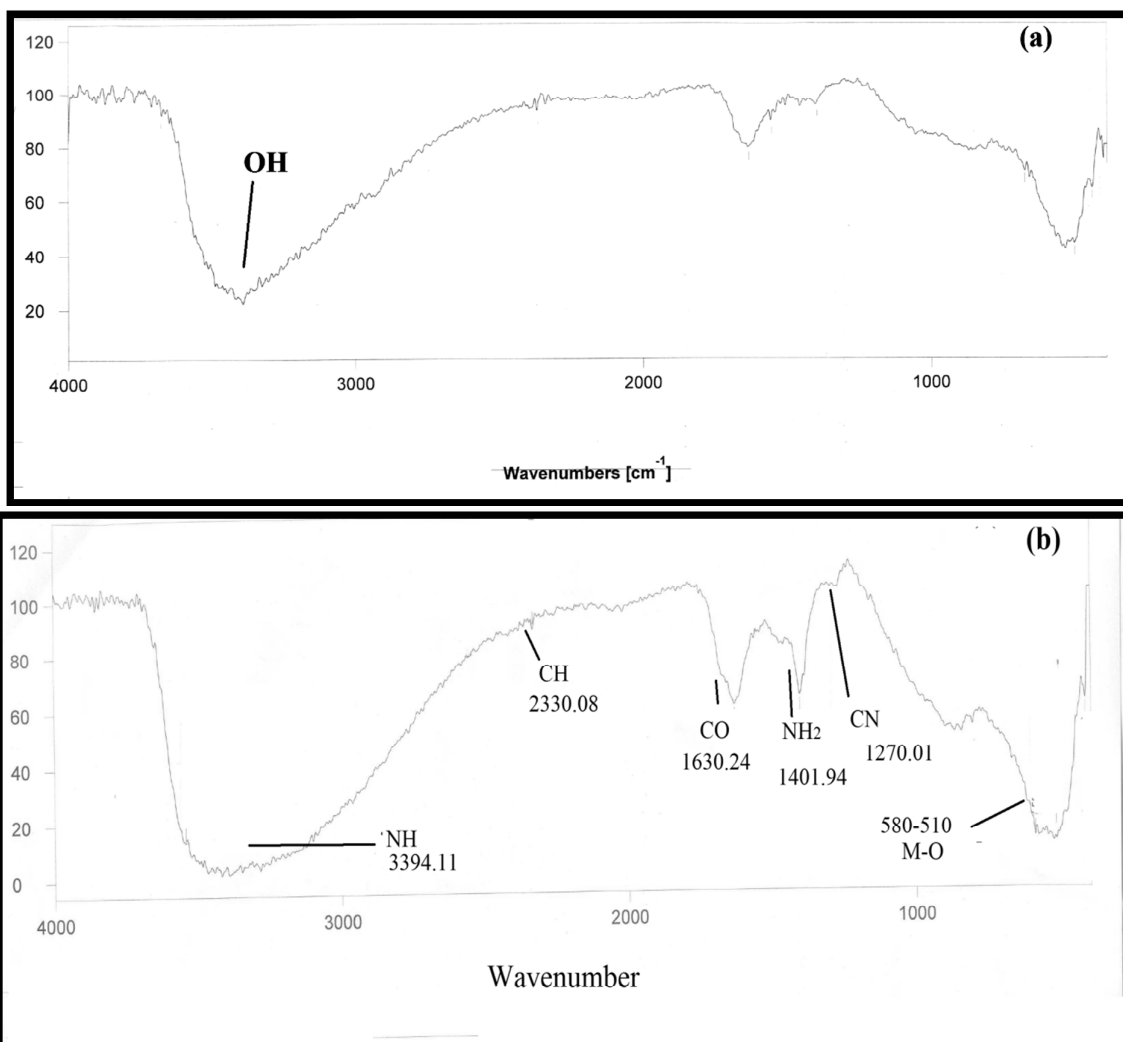


Fig. 1. FT-IR spectrum of (a) Chromium oxide, (b) Polyacrylamide chromium oxide.

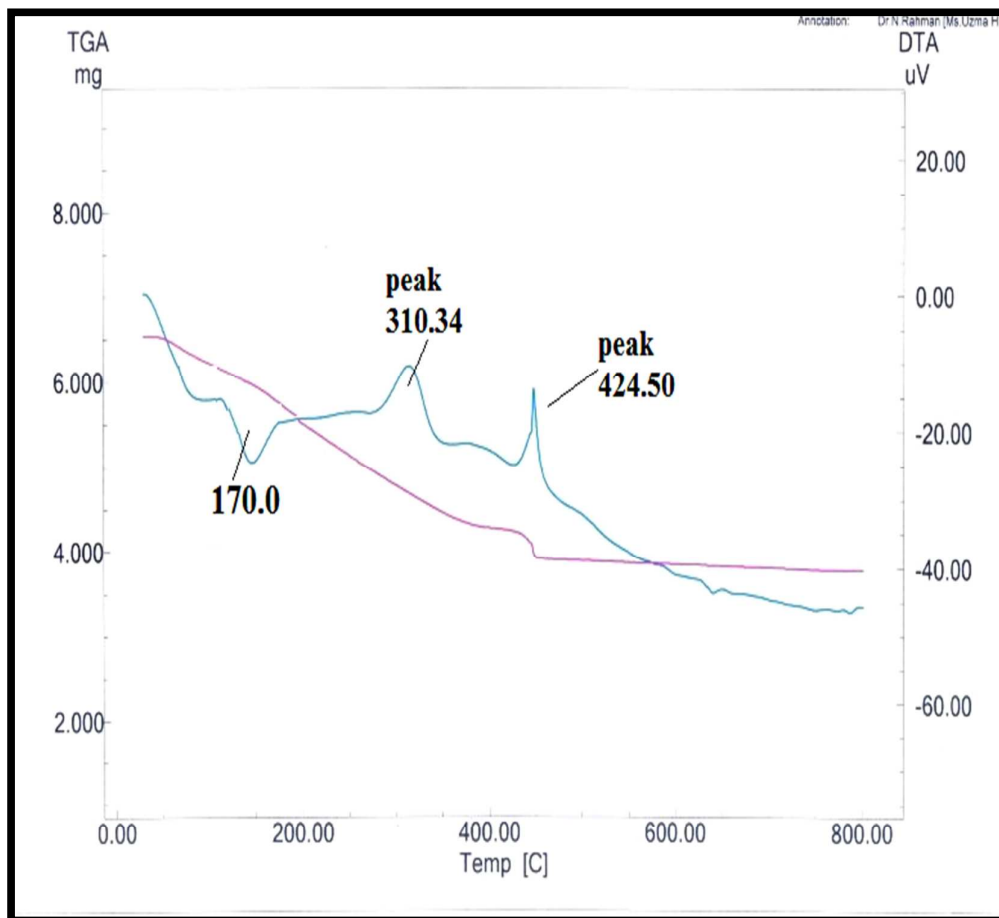


Fig. 2. TGA-DTA curve of polyacrylamide chromium oxide.

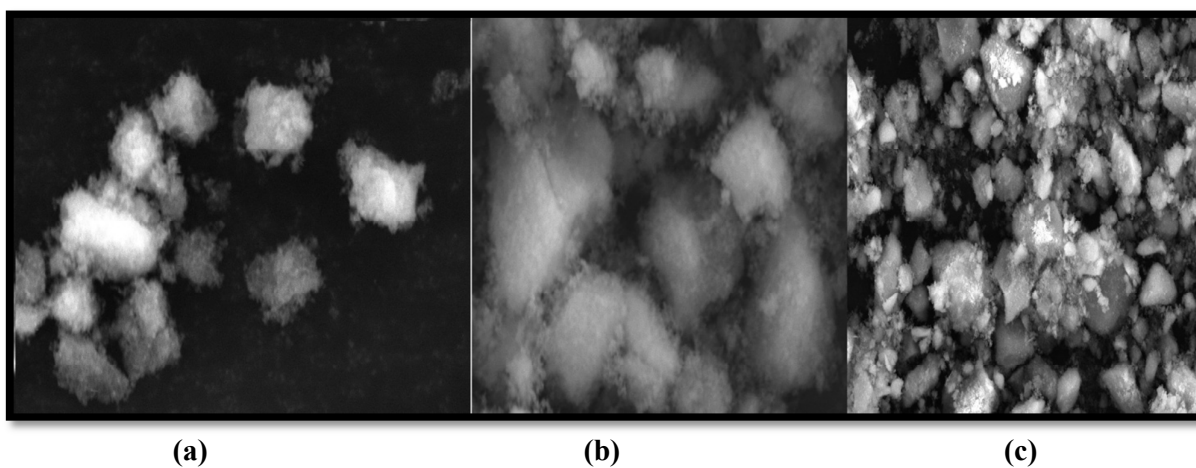


Fig.3. Scanning electron micrographs (SEM) (a) hydrous chromium oxide(HCO) and (b) polyacrylamide chromium oxide and (c) polyacrylamide chromium oxide As(III) loaded material.

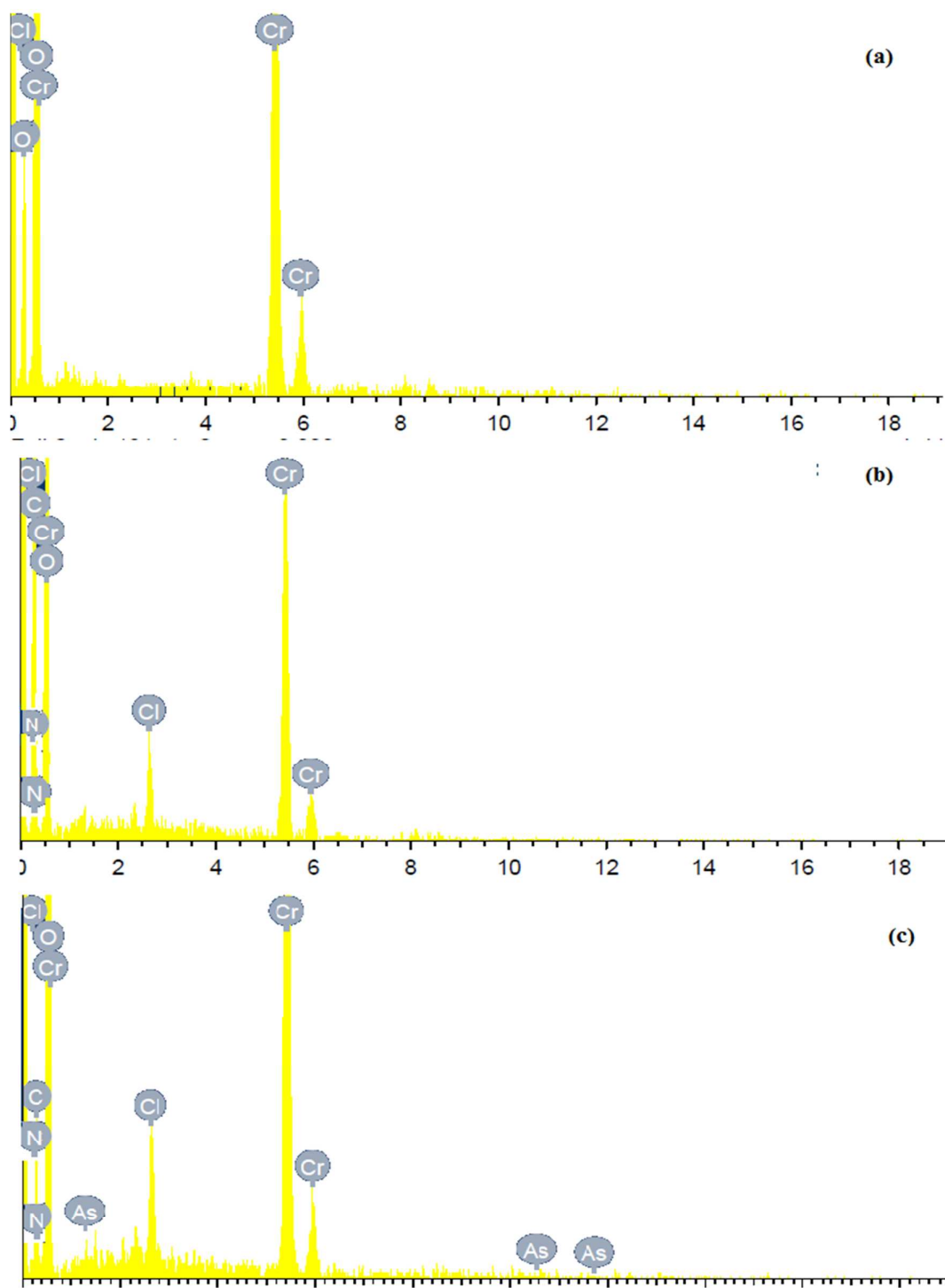


Fig.4. EDX spectrum of (a) hydrous chromium oxide, (b) polyacrylamide chromium oxide, and (c) As (III) sorbed PACO.

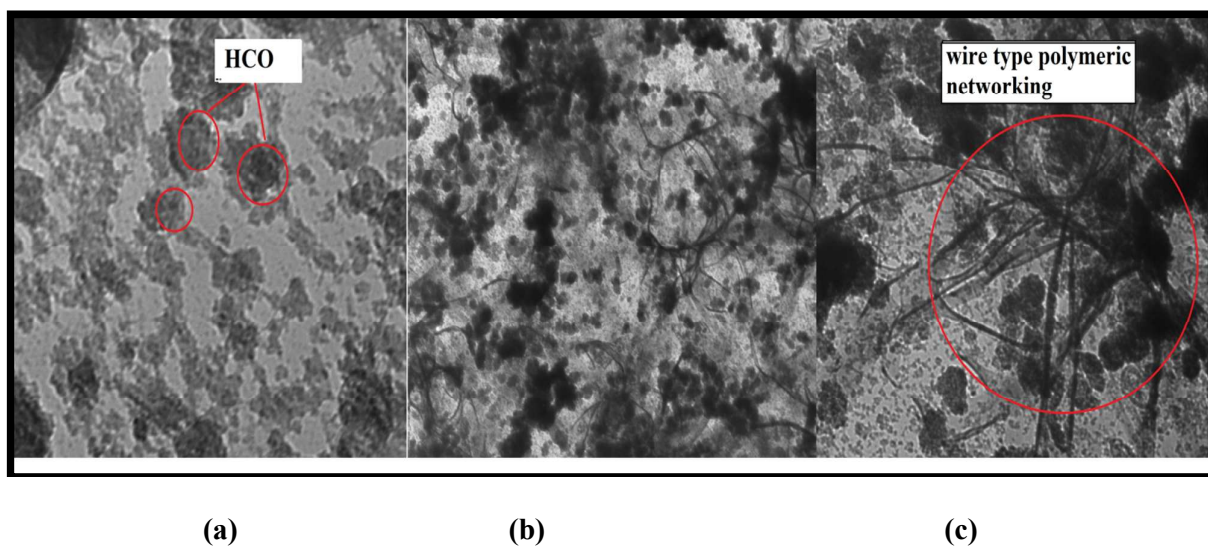


Fig. 5. TEM images; (a) hydrous chromium oxide, (b) As (III) loaded hybrid material, (c) wire type polymeric networking of polyacrylamide on hydrous chromium oxide surface.

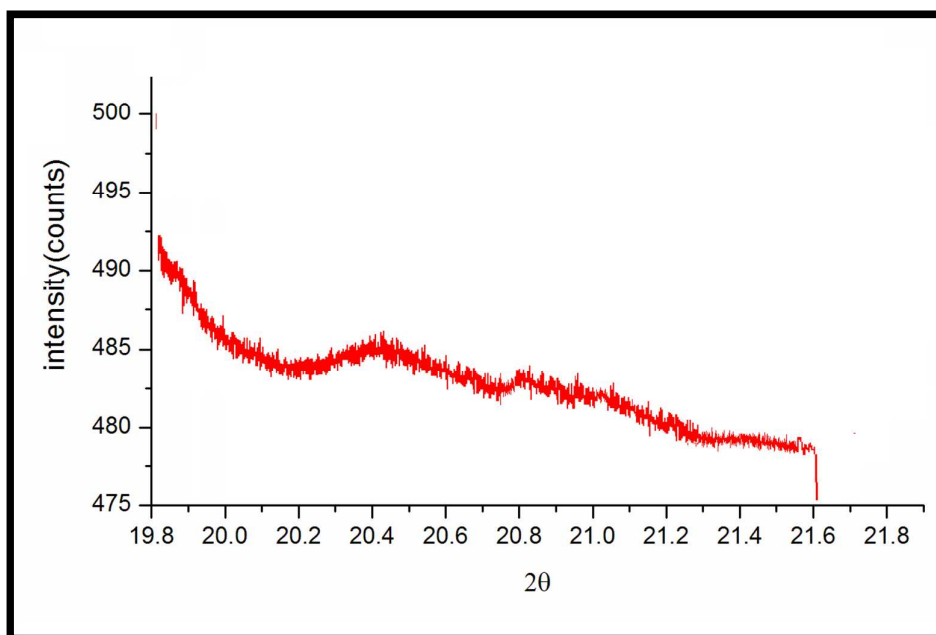


Fig. 6. XRD of Polyacrylamide chromium oxide material.

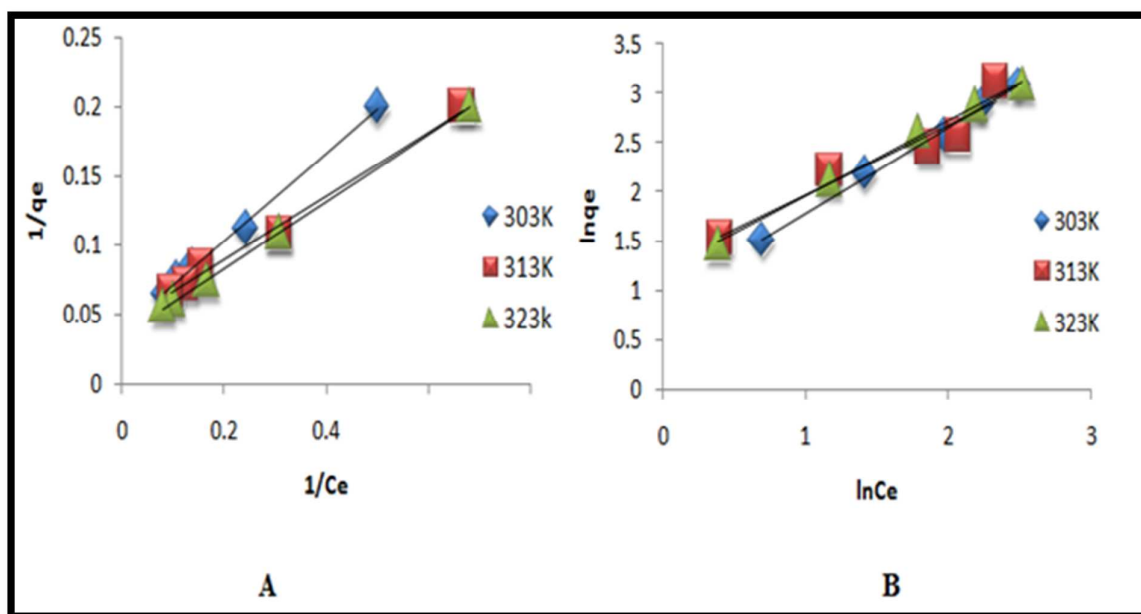


Fig. 7 : (A) Langmuir, (B) Freundlich, isotherm plots for adsorption of As (III) onto PACO;

(Dosage of adsorbent, 0.2 g, contact time, 45 min, pH=6.8; volume, 50 mL)

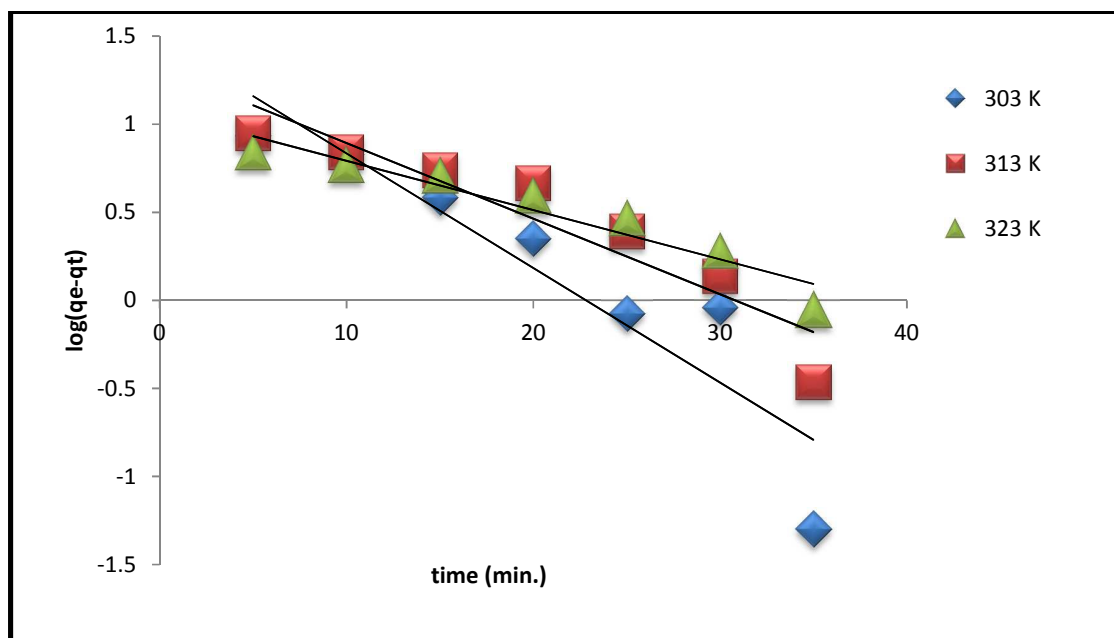


Fig. 8. Pseudo- first order kinetic model for As (III) adsorption on polyacrylamide chromium oxide at different temperature.

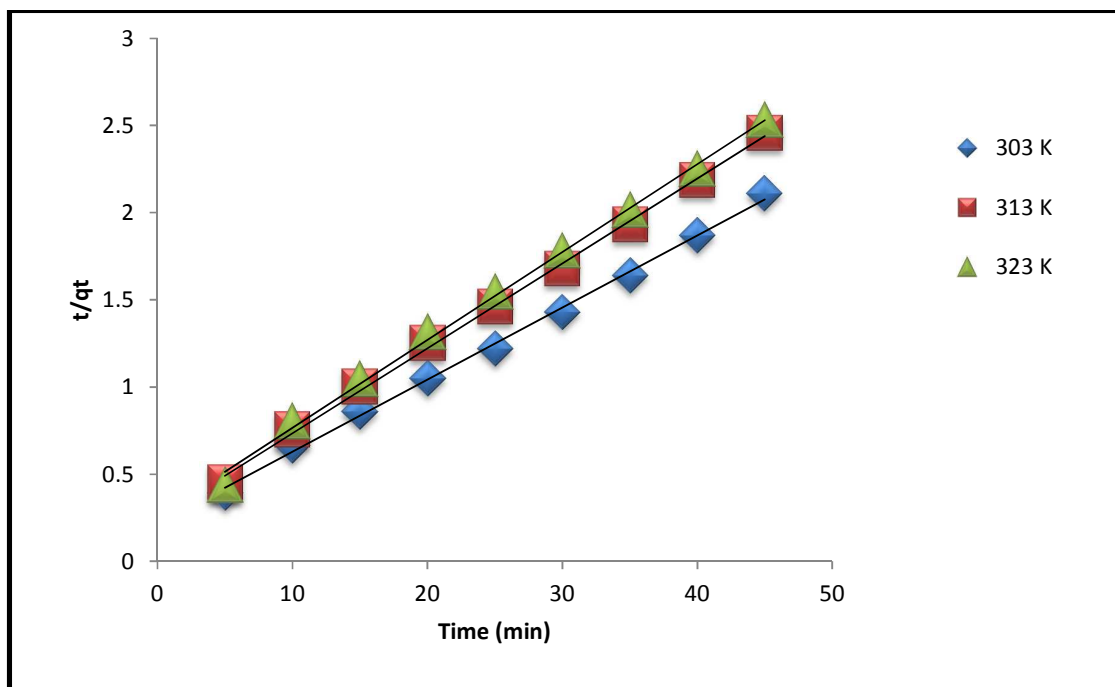


Fig. 9. Pseudo-second order kinetic model for As (III) adsorption on polyacrylamide chromium oxide at different temperature.

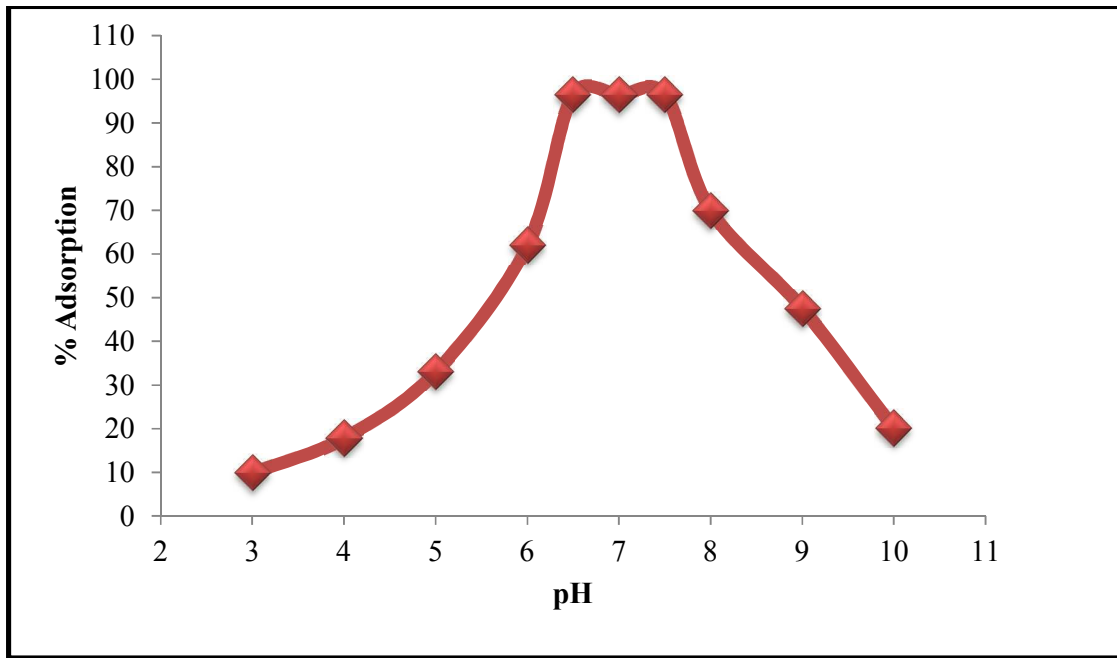


Fig.10. Effect of pH on the sorption of As (III) onto PACO.

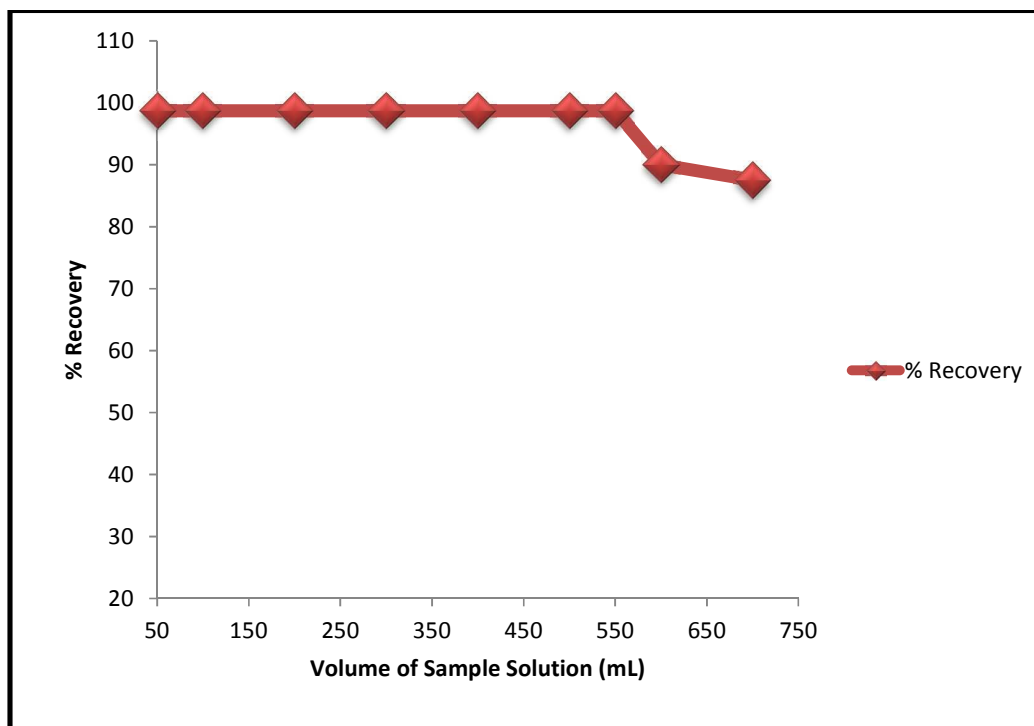
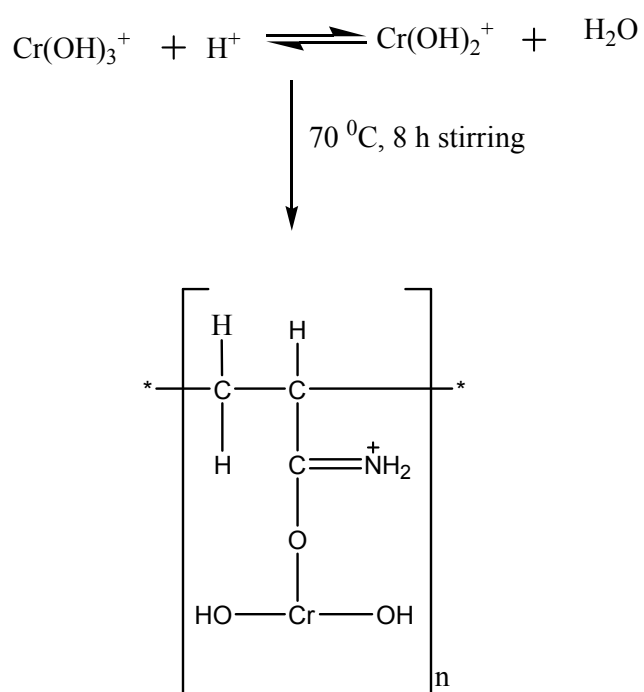
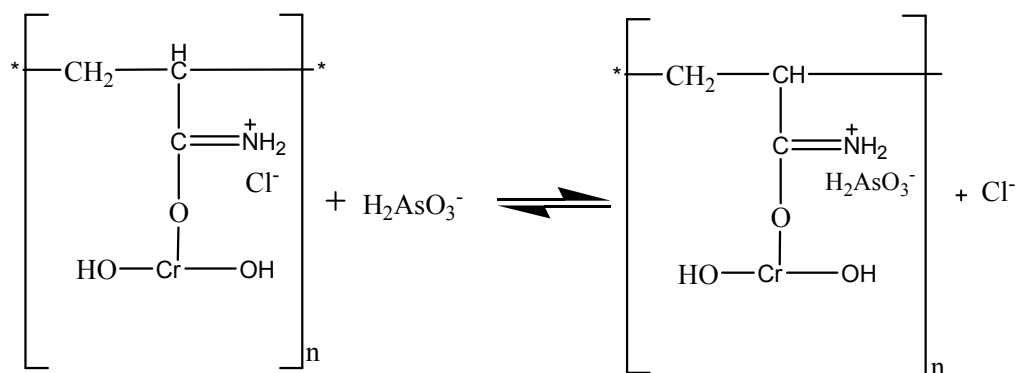


Fig.11. Effect of sample volume on recoveries of arsenic. Concentration; $10 \mu\text{gL}^{-1}$, pH; 6.8. flow rate 3.5 mL min^{-1} .

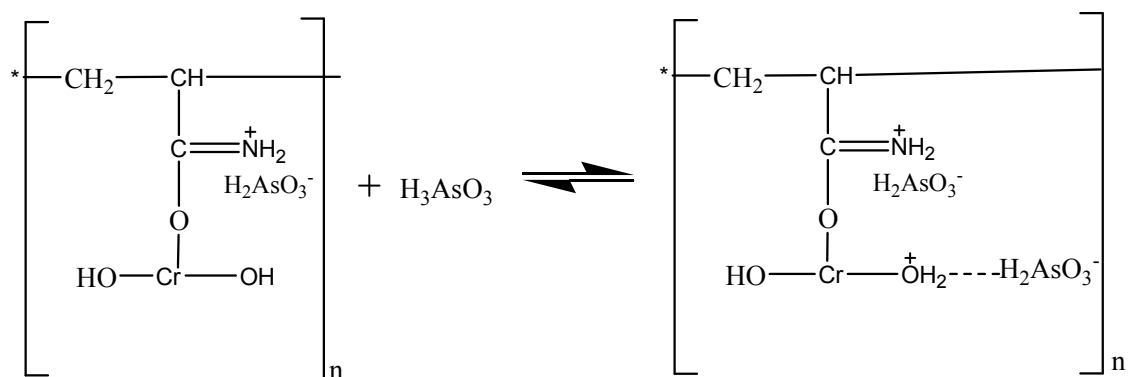


Scheme 1. Formation of polyacrylamide chromium oxide hybrid material under optimal synthesis conditions.

Step I:



Step II:



Scheme 2. Sorption mechanism of As (III) onto PACO.

Table Caption:

Table 1. Experimental conditions of synthesis and ion exchange capacity of polyacrylamide chromium oxide.

Table 2. Different parameters obtained from plots of isotherm models for adsorption of As (III) on PACO.

Table 3. Comparison of the pseudo first-order, pseudo second-order, kinetic model parameters for the adsorption of Arsenic (III) on to PACO, the calculated and experimental q_e values at different temperature.

Table 4. Effect of Interfering Ions on the Recovery of As (III).

Table 5. Day to day and column to column precision.

Table 6. Determination of As (III) in real samples after preconcentration by ICP-AES.

Table 7. Comparison of q_m maximum adsorption capacities for As (III) adsorption with those reported in literature.

Table 1. Experimental conditions of synthesis and ion exchange capacity of polyacrylamide chromium oxide.

Sample Name	Condition of synthesis					
	Chromium(III) Chloride 0.2M(ml)	Ammonium hydrous oxide (6%)	Acrylamide 0.2M (ml)	Final pH	Temperature	Ion-Exchange capacity for Cl ⁻ (meq/g)
PACO	500	until pH 6.0	100	6.0	70±2°C	1.46
PACO-1	500	-	200	6.0	70±2°C	1.45
PACO-2	500	-	300	6.0	70±2°C	1.46
PACO-3	500	-	400	6.0	70±2°C	1.46
PACO-4	500	-	500	6.0	70±2°C	1.46
HCO	500	-	n.a.	6.0	70±2°C	0.70

n.a.= not added

Table 2. Different parameters obtained from plots of isotherm models for adsorption of As (III) on PACO.

Isotherms	Temperature	Parameters			
		K_L (L mg ⁻¹)	q_m (mg g ⁻¹)	R^2	
Langmuir	303K	0.123	25.64	0.997	
	313K	0.175	23.80	0.998	
	323K	0.188	22.72	0.999	
Freundlich		Parameters			
		K_F	n	q_m (mg g ⁻¹)	R^2
	303K	3.49	1.40	18.3	0.923
	313K	3.26	1.30	21.62	0.996
323K	2.47	1.14	22.43	0.997	

Table 3. Comparison of the pseudo first-order, pseudo second-order, kinetic model parameters for the adsorption of Arsenic (III) on to PACO, the calculated and experimental q_e values at different temperature.

Temp.	Pseudo First order kinetic model				Pseudo Second order kinetic model			
	$q_e(\text{exp.})$ (mg/g)	k_1 (L/min)	$q_e(\text{cal.})$ (mg/g)	R^2	k_2 (g/mg/min)	$q_e(\text{cal})$ (mg/g)	h (mg/g/min)	R^2
303K	21.30	0.101	16.29	0.848	0.0079	21.07	2.70	0.997
313K	21.88	0.096	20.94	0.875	0.0075	21.12	4.14	0.997
323K	22.42	0.066	11.77	0.916	0.0055	21.19	4.31	0.998

Table 4. Effect of Interfering Ions on the Recovery of As (III)

Interfering Ions	Concentration of the interfering ions ($\mu\text{g/L}$)	Recovery (%)
K^+ ,	1000	100.5
Na^{2+}	1000	96.0
Cu^{2+}	1000	100
Zn^{2+}	1000	100
Ca^{2+}	1000	99.6
Mg^{2+}	1000	99.1
Cl^-	110	100.2
PO_4^{3-}	400	99.5
CO_3^{--}	250	100
SO_4^{--}	150	99.3

Table 5. Day to day and column to column precision.

Parameters	As (III)	(%) Recovery	As (III)	(%) Recovery
Concentration of standard ($\mu\text{g/L}$)	$6 \mu\text{gL}^{-1}$		$10 \mu\text{gL}^{-1}$	
Day to day precision				
Mean	5.88	98.0	9.84	98.4
Standard deviation	0.23		0.27	
RSD(%)	3.91		2.74	
Column to column precision				
Mean	5.93	98.8	9.67	96.7
Standard deviation	0.27		0.33	
RSD(%)	4.55		3.46	

Table 6. Determination of As (III) in real samples after preconcentration by ICP-AES.

S. No.	Samples	Added (μgL^{-1}) As (III)	Found (μgL^{-1}) As (III)
1.	Tap Water	-	ND
		8.0	7.74 \pm 0.32
2.	River Water	-	4.34 \pm 0.28
		6.0	9.95 \pm 0.31
3.	Basmati rice (unpolished)	-	1.76* \pm 0.12
4.	Basmati rice (polished)	-	2.89* \pm 0.15
5.	Tobacco (cigarette)	-	4.0* \pm 0.17

* $\mu\text{g/g}$, ND = not detected

Table 7. Comparison of q_m maximum adsorption capacities for As (III) adsorption with those reported in literature.

Adsorbents	Initial pH	q_m(mg/g)	Ref.
Nanoscale zero-valent iron (NZVI)	7.0	2.47	[54]
Iron hydrous oxide coated alumina	6.62-6.74	7.64	[55]
Titanium dioxide-loaded Amberlite XAD-7 resin	5-10	9.74	[56]
Leonardite char	7.0	4.5	[57]
Fe₃O₄-Honeycomb briquette cinders composite	7.0	3.07	[58]
Magenetic wheat straw	7.0	3.8	[59]
Fe₃O₄-RGO nanoparticles	7.0	13.1	[60]
Fe₃O₄-RGO-MnO₂ nanoparticles	7.0	14.04	[61]
NZVI-activated carbon nanoparticles	7.0	18.2	[62]
Polymer supported Mn/Fe oxides	3.3-5.0	13.5	[63]
PACO	6.8	22.48	This work